High efficiency electrochemical adsorption enhanced reduction of low concentration triiodomethane

Wenke Niu[a], Zihao Guo[a], Qingwei Wang[a], Xiaojun Hu[a,*], Guohua Zhao[b,*], Fuxiang Tian[a], Jingxian Jiang[a], Jibo Liu[a], Hongbo Zhang[a]

[a]*School of Chemical and Environment Engineering, Shanghai Institute of Technology 100 Haiquan Road, Shanghai 201418, China, emails: hu-xj@mail.tsinghua.edu.cn (X. Hu), 2606465835@qq.com (W. Niu), 405083885@qq.com (Z. Guo), wangqw@sit.edu (Q. Wang), 13916841275@163.com (F. Tian), jxjiang@zju.edu.cn (J. Jiang), jiboliu@sit.edu.cn (J. Liu), hongbo_zhang888@163.com (H. Zhang)*
[b]*School of Chemical Science and Engineering, Tongji University, 1239 Siping Road, Shanghai 200092, China, email: ghzhao@tongji.edu.cn*

ABSTRACT

The highly efficient electrochemical (EC) reduction of triiodomethane (TIM) was investigated on a Cu nanoparticles (NPs) modified activated carbon fiber (Cu/ACF). The electrochemical adsorption for TIM over Cu/ACF electrode was investigated, and the removal of TIM increased from 69% to 99% with increasing the from –0.3 to –1.0 V in the absence of a cathode potential, which is more efficient than with pure fluorine doped tin oxide coated glass (FTO) electrode, ACF electrode and Cu/FTO electrode. The removal efficiency of TIM was strongly dependent on the electrochemical adsorption as the applied potential was lower than –1.0 V. Due to the catalytic ability of Cu nanoparticles, the reduction efficiency was changed with the presence of Cu nanoparticles. The rate constant, k, was firstly increased from 0.39 to 1.78 h^{-1} as the Cu loading amount increased from 0.02 to 0.54 mg/cm^2. However, the constant k was then decreased to 1.39 h^{-1} as the Cu loading amount further increased to 0.81 mg/cm^2. The Cu nanoparticles played a significant role in forming atomic H* to realize indirect TIM reduction.

Keywords: Electrochemical reduction; TIM; Activated carbon fiber; Electrochemical adsorption

1. Introduction

With the development of industry and population growth, water pollution has become increasingly serious in the past decades. For supplying clean water, chlorination was the most commonly used disinfection method to eliminate the potential pathogenic microorganisms and organic pollutants. It is now well-established from a variety of studies that various disinfection by-products (DBPs) were formed by the reaction of the disinfectant with naturally occurring organic matter during the disinfection process [1]. In the United States and Canada, a survey demonstrated that the I-DBPs such as iodine-containing haloacetic acids (I-HAAs) and iodine-containing trihalomethanes (I-THMs) were detected in chlorination treated water. It has previously been observed that with the presence of iodide, chloramine oxidization can produce free iodine species (e.g., HOI, OI$^-$, I$_2$, I^{3-}, and so on), which further convert to dissolved organic matter (DOM) into I-DBPs [2–7]. In the last 40 y, more than 500 detrimental DBPs had been identified [8], including various I-THMs and I-HAAs in the water purification process. In addition, as emerging DBPs such as I-THMs were identified in waters and shown to be more cytotoxic than chlorinated and brominated THMs [9–12], there are also increasing concerns toward these new I-THMs. Previous studies have demonstrated that

* Corresponding authors.

triiodomethane (TIM) was 60 and 146 times more cytotoxic than $CHBr_3$ and $CHCl_3$, respectively [6]. In fact, it is due to the formation of iodoform which has low odour (0.02 μg/L) and taste (5 μg/L) threshold concentrations [9]. This could explain the reported nuisance arising from the low concentration of I-THMs that are able to cause strong offensive odors and taste in drinking water. Thus, it is highly desirable to develop effective treatment methods to remove I-DBPs.

Currently, only a few studies have reported the formation and fate of I-THM during the treatment of water and wastewater due to the higher difficulty in detection [13,14]. In addition, in view of the I-DBPs concentration in water is in micrograms per liter level, it is difficult to remove I-DBPs absolutely. In these studies, conventional water treatment processes (such as sedimentation, ozonation, and direct UV photolysis) were not effective in the removal of I-THMs. As the typical advanced technologies, membrane filtration and reverse osmosis (RO) were efficient for I-THMs removal but still facing some insurmountable difficulties such as complex equipment, high cost, and so on [15,16]. Therefore, exploring simple and effective techniques to realize the degradation of I-THMs is in urgent need. Under the circumstances, advanced oxidation processes supplied efficient processes in I-DBPs degrading [17].

In recent years, electrochemical reductive treatment has been recognized as a promising method for reduction of DBPs [18–22]. There has been an increased interest in environmental applications of electrochemical processes, which are chemical-free, electricity-driven, highly efficient and selective, and easy to realize automatic operation [23–27]. Combinations of electrochemical reductive treatment and sorption on activated carbon fiber (ACF) as well as other processes allow the removal of as much as 70% of Cl^- and Br^- containing THMs and ca. 60% of HAAs [28,29]. Therefore, using electrochemical adsorption to enhance electrochemical reduction process will become a possible efficient method for low concentrations I-DBPs removing. The compact reactor size, minimal formation of by products and low maintenance requirements of the electrochemical process make it highly attractive in drinking water treatment [30]. This method ensures the selective removal of halogen atoms from DBPs without producing any other toxic byproducts or adding any toxic chemicals [31–33]. Simultaneously, in order to enrich low-concentration pollutants, ACF is used as the substrate electrode owing to its excellent electrical conductivity, large specific surface area, porous structure, and low cost, which creates favorable conditions for I-DBPs removing. The porous structure can provide an outstanding platform for target pollutants adsorption, which is beneficial for the increase of the pollutant concentration on the surface of the catalytic electrode. And at the same time, it also enlarges the effective contact area between the catalytic electrode and the pollutant.

However, it was insufficient for pollutant degradation only with the present of ACF substrate electrode due to the deficiency of atomic H*. It is recognized that the reduction of contaminants at cathode surfaces may occur through both direct and indirect mechanism. Direct reduction occurs by electron tunneling, and indirect reduction of contaminants occurs via reaction with atomic hydrogen adsorbed on the cathode. Namely, direct dehalogenation by electron transfer and an indirect process induced by atomic H*, take place during the electrocatalytic reduction process [34]. Generally, in contrast to the low reduction efficiency of electron transfer, the catalytically produced atomic H* plays a predominant role in dehalogenation. Thus, the fabrication of suitable catalysts that can produce higher amounts of atomic H* has great potential for practical applications. Wang et al. [35] deduced that H_2 was decomposed into atomic H* for dehalogenation reaction. However, relatively little literature was available on the intermediates and degradation pathway of direct and indirect reductive dehalogenation of TIM at the cathode. Therefore, precious metals such as Pb and Ag have long been used as electrode material [36,37]. For example, Bonin et al. [38] exhibited that Pd-modified cathodes had high dechlorination efficiencies for chlorinated organics, as Pd can activate H_2 as well as catalyze the electrochemical reduction of H^+ or H_2O to produce continuously adsorbed nascent H* [39]. However, the precious metal facilitates the hydrogen evolution reaction of the cathode during the electrochemical process at a high reduction potential, resulting in a decrease in electrochemical reduction efficiency. Therefore, it is necessary to find a non-noble metal catalyst with excellent catalytic performance. In recent years, low-cost copper electrode has been found to exhibit good catalytic activity in EC reduction process [40], which can be driven by the electrons transferring to Cu [41]. In addition, different deposition conditions can promote the formation of different crystal faces in order to better regulate the electrochemical reduction reaction. Therefore, we constructed a Cu nanoparticle-loaded ACF electrode for electrochemical reduction degradation of TIM. The synergistic effect of electrochemical adsorption, electrochemical reduction and Cu catalysis is more conducive to the efficient removal of I-DBPs.

Hence, the high-efficiency electrochemical reduction of TIM on Cu/ACF electrodes was investigated to reveal the possible removal mechanisms. The influences of different reduction potentials on the electrochemical behavior of the TIM, and the effect of Cu particle deposition conditions on the adsorption enhancement of the TIM on ACF surfaces were mainly explored. The physical adsorption removal rate of the Cu/ACF reached 29% at 2.5 h without reduction potential applied on the electrode. When a reduction potential was applied to the working electrode, the electrochemical adsorption removal efficiency of the TIM increased from 69% to 80%. Under the same conditions, the catalysis of Cu nanoparticles deposited on the working electrode increased the removal rate of TIM to 99%. TIM reduction at different cathode potentials, pH values and Cu loading amounts were also investigated. Therefore, a Cu nanoparticle-loaded ACF electrode was constructed for electrochemical degradation of TIM. Simultaneously, the possible degradation pathway and reduction mechanism of TIM were involved.

2. Experimental methods

2.1. Reagents and chemicals

Chemicals were AR grade unless otherwise mentioned. All solutions were prepared using Milli-Q water (Millipore Corp., USA). TIM were purchased from Sinopharm Chemical

Reagent Co., Ltd., (Shanghai, P.R. China) The stock solution of TIM was prepared by dissolving 0.05 g TIM in 0.05 L methanol solution (1.00 g/L). The 10 μg/L TIM solution was diluted from TIM stock solution using DI water. All stock solutions were stored at 4°C in a refrigerator. High performance liquid chromatography (HPLC) grade methanol was purchased from Merck (Singapore). For quantitative chromatographic analysis, stock standard solutions were prepared in methanol by weighing approximately 0.5 mg of individual neat TIM into a 50 mL volumetric flask and diluting to volume. The secondary standard solutions were prepared by dilution of the primary standard to 10 μg/L.

2.2. Preparation of ACF-Cu electrode

For this study, carbon fiber fabric was prepared using continuous carbon fiber. The carbon fiber bundle (TR50S12L, Mitsubishi Chemical Co., Ltd., Tokyo, Japan), which has 12,000 filaments and the diameter of each fiber is 7 μm, was used. Tensile strength and elastic modulus of carbon fiber were 4.90 and 240 GPa, respectively. Additionally, the carbon fiber plain weave (TR3110MS, Mitsubishi Chemical Co., Ltd., Tokyo, Japan) was used for the substrate.

Prior to the electrochemical experiment, the ACF were cleaned in acetone and ethanol by ultrasound, followed by burning the samples in the fire, which can increase the specific surface area and provide an effective place for depositing Cu particles. The samples were soaked in 0.5 M NaOH and 0.5 M H_2SO_4, respectively, and then dried in air and heat-treated at 350°C for 30 min. ACF filling Cu were decorated by a galvanostatic method under high current conditions. The electrodepositions were carried out in a conventional three-electrode system using CHI 760d with the electrolytes solution containing 0.02 M $CuCl_2$ and 0.01 M KCl at room temperature. And then the pH value of the solution was adjusted to 7.00 by NaOH. An electrodeposition approach was rationally designed with a constant current density of 50 mA/cm^{-2}. To obtain a uniform deposition of Cu into the ACF, the operations performed at different deposition potentials and times were investigated.

2.3. EC reduction experiment

EC reduction experiments were performed using a 100 mL cylindrical glass reactor filled with 100 mL of fresh ITHMs aqueous solution at room temperature. Electrochemistry reduction of TIM (its initial concentration is 10 μg/L) in DI water under different reduction potential was conducted in triplicate. Aliquots were sampled at predetermined time intervals and analyzed immediately by purge-and-trap coupled with gas chromatography–mass spectrometry (GC/MS).

2.4. Electrochemical analysis

A reliable and sensitive method for ITHMs determination at μg/L level in water sample was developed using automatic purge-and-trap (P&T) extraction (Tekmar, Atomx) coupled with GC (Agilent, 6890A)/MS (Agilent, 5973C). A DB-624 column (J&W) with helium as the carrier gas was used. The oven temperature program was as follows: 45°C

for 2 min, then increased at a rate of 10°C/min to 100°C, held at 100°C for 2 min, then ramped up to 200°C at 5°C/min, to 250 at 20°C/min, and held at 250°C for 5 min. Selective ion monitoring (SIM) mode was operated in MS for quantitative analysis of ITHMs. Total organic carbon (TOC) was analyzed by a TOC analyzer (Shimadzu, TOC-VCSH). EC reduction of I-THMs was measured by an electrochemical workstation (CHI 760d).

2.5. Characterization

The morphology and microstructure of Cu/ACF electrodes were characterized by scanning electron microscopy (SEM, SU8010, Japan). All EC measurements were performed on a CHI 760D electrochemical workstation (CH Instruments, Inc., USA) using a conventional three-electrode system with the as-prepared electrode as the working electrode, Ag/AgCl as the reference electrode and a platinum foil as the counter electrode in 0.1 M KCL aqueous solution.

3. Results and discussion

3.1. Excellent EC adsorptive property of Cu/ACF

The adsorption of the cathode for pollutant was the first step for pollutant removing. The adsorption for pollutants rooted from the porous structure of ACF and the enhancement of electrochemical adsorption. The "*I–t*" method under varying potential was employed to investigate the enhancement of electrochemical adsorption. The adsorption of TIM changing over time on the surface of the working electrode with the absence of applied voltage was examined (as shown in Fig. 1a). Without potential applying, the TIM concentration in the solution was decreased rapidly at the beginning of 1.5 h due to the excellent adsorption of ACF substrate electrode. Then, the TIM concentration reached a steady-state. Simultaneously, the adsorption amount of ACF substrate electrode was twice than FTO which further indicated the porous structure of ACF for TIM physical adsorption. After the Cu was deposited on ACF substrate, the TIM removing was 20% higher than that without Cu deposition.

To evaluate the effect of the applied potential, the potential influenced TIM electrochemical adsorption was investigated as the potential changed from –0.2 to –1.2 V. Added 1 mL TIM stock solution to the electrochemical reaction solution every 100 s at different applied potentials and the changes of the "*I–t*" curve were recorded. As shown in Fig. 1b, as the applied voltage varied from –0.1 to –0.9 V, the "*I–t*" curve had no obvious fluctuation with the TIM addition. When the applied voltage was higher than –1.0 V, the "*I–t*" curve began to fluctuate with the addition of TIM. The result indicated that the electrochemical adsorption of TIM converted into electrochemical adsorption and electrochemical reduction simultaneously as the applied voltage reaching the reduction potential. The inset shows that with the increase of the applied voltage (–0.2 to –0.8 V), the electrochemical adsorption of TIM was greatly enhanced and the maximum adsorption amount was achieved at the voltage of –0.8 V. It suggested that a higher voltage was favorable for TIM electrochemical adsorption. As the
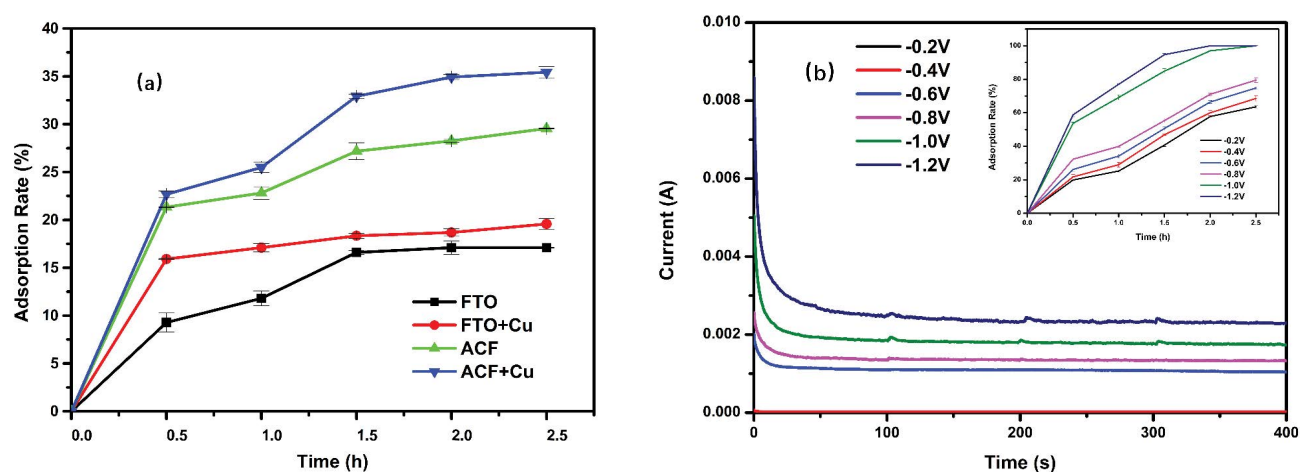
Fig. 1. Effect of (a) the material itself on the physical adsorption properties of TIM without the application of potential and (b) different voltages on the TIM in the "*I–t*" curve. The illustration was the electrochemical adsorption of TIM by different potentials until EC reduction.

potential increased from –0.8 to –1.0 V, the total removal efficiency of TIM has been greatly improved at 2.5 h indicating that the TIM reduction began at –1.0 V.

The TIM concentrations of samples were detected using GC (Agilent, 6890A)/MS (Agilent, 5973C). The TIM removal efficiency was calculated according to the Eq. (1):

$$\text{TIM removal efficiency}(\%) = \frac{(\text{TIM}_0 - \text{TIM}_t)}{\text{TIM}_0} \times 100\% \quad (1)$$

where TIM_0 is the influent concentration (μg/L), TIM_t is the concentration (μg/L) at time *t*.

3.2. EC reduction performance of TIM

In the excellent electrochemical adsorption-enhanced reduction of TIM, the reduction potential applied on the surface of the working electrode plays an indispensable role in TIM degradation. Electrochemical reduction of TIM on the Cu/ACF electrode at different applied potentials was investigated and the results are shown in Fig. 2a. The removal efficiency of TIM increased with the increase in the reduction potential. Within 2.5 h, the TIM removal efficiency changed from 69% to 80% when the reduction potential increased from –0.3 to –0.9 V. TIM removal was greatly enhanced and the efficiency reached 99% at –1.5 V under other conditions that remained unchanged. Further increasing the applied bias potential to –1.9 V did not improve the removal efficiency.

The kinetic analysis of the data in Fig. 2a gives an average correlation coefficient for the ln[TIM] vs. *t* plot in the linear region of 0.995, suggesting the suitability of the pseudo-first-order reaction kinetics used to fit TIM reduction. The pseudo-first-order reaction kinetics was used to fit the TIM removal process as a function of the reaction time. The model is given by Eq. (2):

$$C_t = C_0 \exp(-kt) \quad (2)$$

where *t* is the reaction time (h), *k* is the rate constant (h^{-1}), and C_0 and C_t are the TIM concentrations (μM) at times of *t* = 0 and *t* = *t*, respectively. As shown in Fig. 2b, the value of *k* increased slowly when the reduction potential was less than –1.0 V. As the potential changed from –1.0 to –1.9 V, the value of *k* rised sharply, and reached a plateau of 1.90 h^{-1} at –1.9 V. Intense and profuse hydrogen bubbles were produced as the potential was over than –1.5 V, simultaneously, the H$_2$ generated on the electrode also caused the passivation of working electrode. Thus, the EC reduction efficiency of TIM decreased at potentials over –1.9 V. As shown in Fig. 2c, the TIM removing efficiency was added apparently following the potential increasing below –0.9 V, while the trend added sharply from –0.9 to –1.8 V. As the potential further rose to over –1.9 V, the TIM removing efficiency had no obvious changing. That might be attributed to the atomic H* generated as the potential changing. Similar to the reduction dehalogenation of chloroacetic acids reported in literatures, the electrocatalytic dehalogenation occurring at potentials less than –1.0 V would evolve the molecular hydrogen [40]. Pd(0) played an important role in the chemisorption and decomposition of hydrogen into atomic H*, which is a highly activated intermediate hydrogen radical. Atomic H* adsorbed on the surface of the electrode at low cathode potentials is beneficial for the electrochemical reduction of TIM.

Moreover, it was reasonable to hypothesize that the relatively low removal efficiency at potentials below –1.0 V was caused by the electrochemical sorption. As the applied potential was less than –1.0 V, the TIM removing might be attributed to the EC adsorption on the Cu/ACF electrode without electrochemical reduction. The TIM desorption from Cu/ACF was carried out to further explore the adsorption mechanism. The TIM desorption efficiency as the potential changed from a low potential of –0.3 V to a high potential of –1.9 V is revealed in Fig. 2d. It can be seen from the figure that the desorption efficiency of TIM gradually increased from –0.3 to –1.0 V. According to Fig. 2a, the larger the potential, the more the TIM was adsorbed.
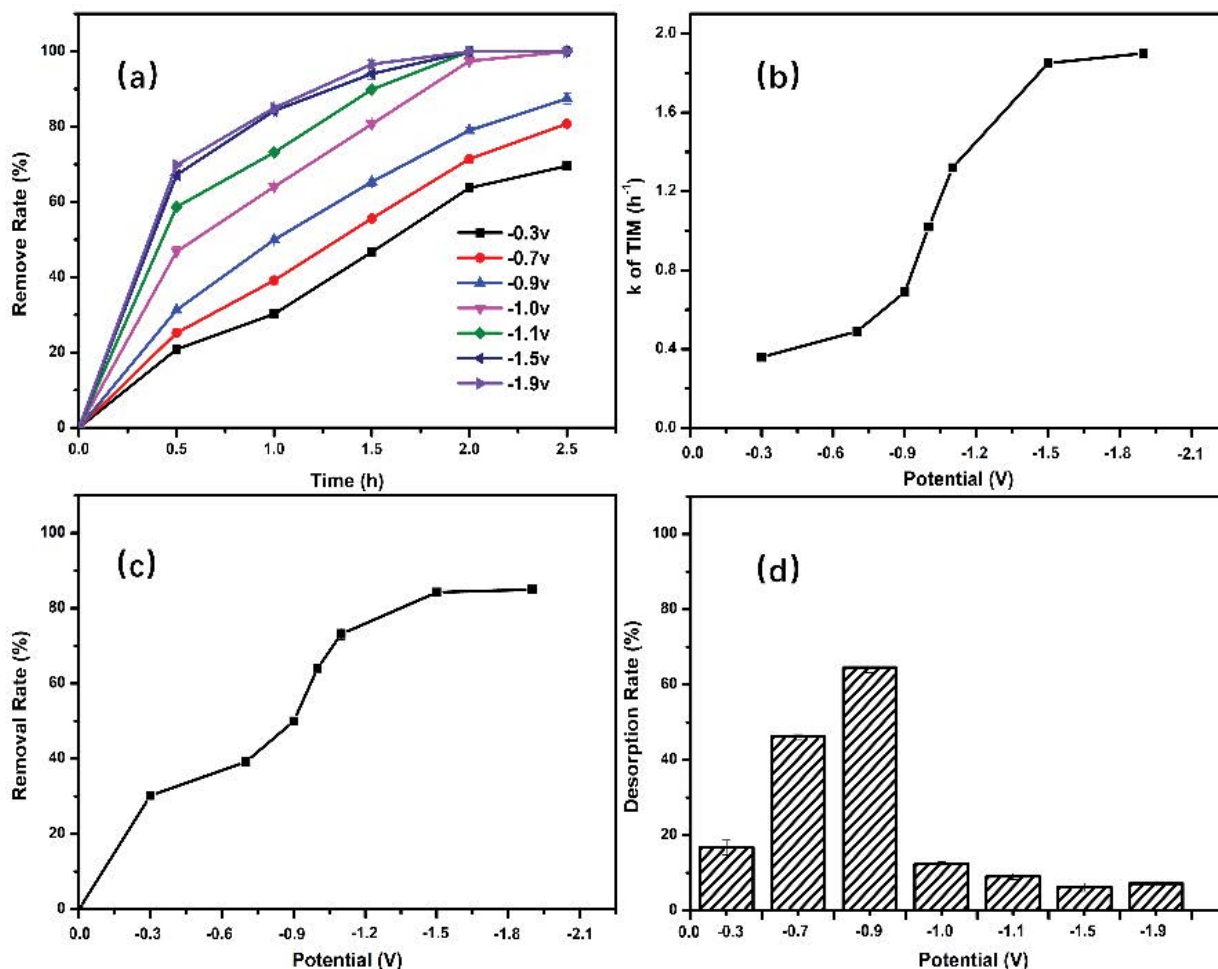
Fig. 2. (a) Electrochemical (EC) reduction of TIM at different applied potentials (filled symbols denote normalized TIM concentration). (b) Effect of applied bias potential on the TIM reduction kinetics at the Cu/ACF electrode at 1 h (1 mM KCl; 10 μg/L initial TIM concentration; Cu loading amount: 0.54 mg/cm²). (c) Effect of applied bias potential at 1 h on the TIM removal efficiency. (d) Desorption efficiency of TIM at different applied potentials.

However, the reduction reaction did not occurr at a potential of –1.0 V or less. Therefore, the adsorption efficiency and the elution efficiency increased gradually along with the increasing in the over potential. From –1.0 to –1.5 V, the elution efficiency of TIM was gradually decreased with the reduction potential further increasing, and the reason might be attributed to the TIM reduction partially.

3.3. High efficiency TIM electrochemical reduction

As an efficient catalyst for TIM reduction, the proper amount of loaded Cu nanoparticles play an significant role in TIM removing. The Cu/ACF electrodes with different Cu loading amounts were characterized by SEM analysis. As presented in Fig. 3a, the bare carbon fibers were comprised of hundreds of carbon fibers. The ample inner space of carbon fiber can provide optimal channels for targeted TIM anions to transfer to the catalytic active sites. Abundant sphere-like electrodeposited Cu nanoparticles dispersed evenly on the carbon fiber as shown in Figs. 3b–d and the diameter of the Cu nanoparticles was around 50 nm.

The effect of Cu loading amount on the TIM deiodination and the corresponding pseudo-first-order reaction rate constant (k, h^{-1}) were investigated due to its crucial role in promoting deiodination efficiency. As shown in Fig. 4a, the rate constant k of TIM removal at the 0.54 mg/cm² Cu/ACF electrode was nearly doubled in comparison to that at the 0.02 mg/cm² Cu/ACF electrode. However, when the loading amount of Cu increased from 0.54 to 0.81 mg/cm², the value of k decreased slightly, suggesting that the electrochemical activity of the Cu/ACF electrode was not proportional to the loading amount of Cu nanoparticles because the ACF was overspread by Cu nanoparticles (Fig. 3d).

As shown in Figs. 4c and d, the influences of different deposition conditions for EC reduction of TIM were further investigated. At the same deposition time of 600 s, the electrochemical removal efficiency of TIM increased with the increase in deposition potential (Fig. 4c). The inset showed the Cu nanoparticles loading amount increased from 0.02 to 0.54 mg/cm² when the deposition potential increased from –0.005 to –0.3 V. A larger Cu nano-particles loading amount caused more electrons generation for H*
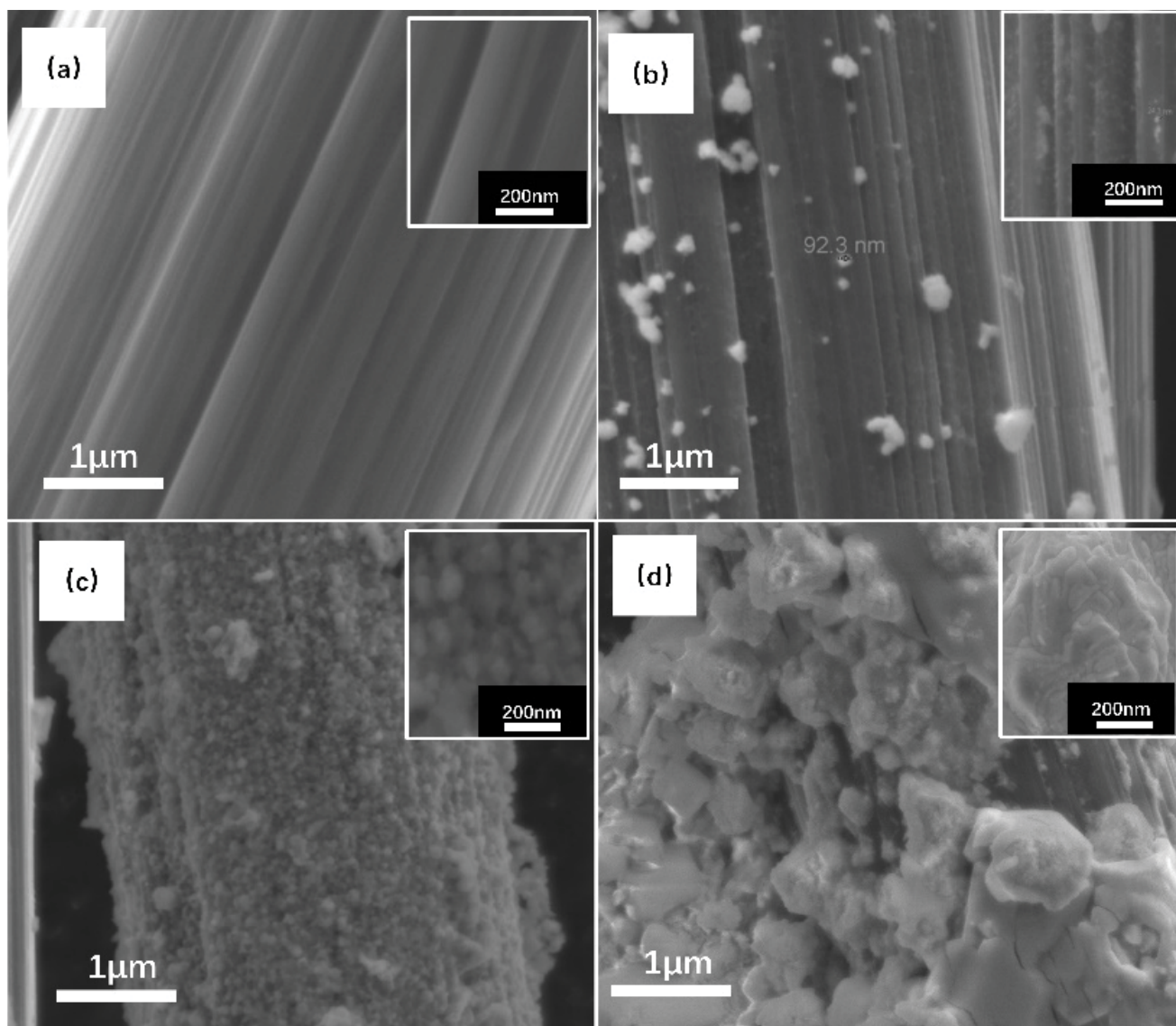
Fig. 3. SEM images of the Cu/ACF electrodes with Cu loading amounts changing. Pure ACF without any Cu nanoparticles loading (a), 0.23 mg/cm² Cu nanoparticles loaded ACF (b), 0.54 mg/cm² Cu nanoparticles loaded ACF(c), and 0.81 mg/cm² Cu nanoparticles loaded ACF (d).

formation, further resulting in a promotion in TIM removing [35]. However, when the deposition potential rose to –0.4 V, the loading amount of Cu was further increased to 0.81 mg/cm², while the removal efficiency of TIM had no obvious changing. It can be attributed to the fact that the Cu nanoparticles form a stack on the surface of the ACF electrode when the deposition potential was raised from –0.3 to –0.4 V, thereby reducing the contact area of the TIM with the Cu particles supported on the surface of the ACF electrode, which further resulted in no significant change or a slight decrease in the reduction efficiency of the TIM.

In addition, when the deposition potential was fixed at –0.3 V, the EC reduction efficiency of TIM was observed to increase gradually as the Cu/ACF deposition time increased from 300 to 900 s (Fig. 4d), and the inset showed the deposition amount of Cu increased from 0.02 to 0.54 mg/cm².

When the deposition time increased from 900 to 1,200 s, the loading of Cu further increased to 0.81 mg/cm² and there was no significant change in the EC reduction efficiency of TIM. The explanation here is the same as above.

At excessive Cu loadings, the similar inhibition of deiodination has been reported in previous literatures, and they attributed this phenomenon to (i) the increased local currents of hydrogen evolution preventing the transfer of targets to electrode surface, and (ii) the decreased active sites due to the Cu accumulation [42,43]. In this study, high Cu loadings may lead to the block of the accessibility of TIM to the interior Cu sites, resulting in the decrease in catalytic efficiency. The result indicated that the unmodified ACF was not an efficient electrode for the reduction of TIM. It can also be deduced that the electrochemical reduction of TIM at –1.0 V occured through direct reduction mechanism.
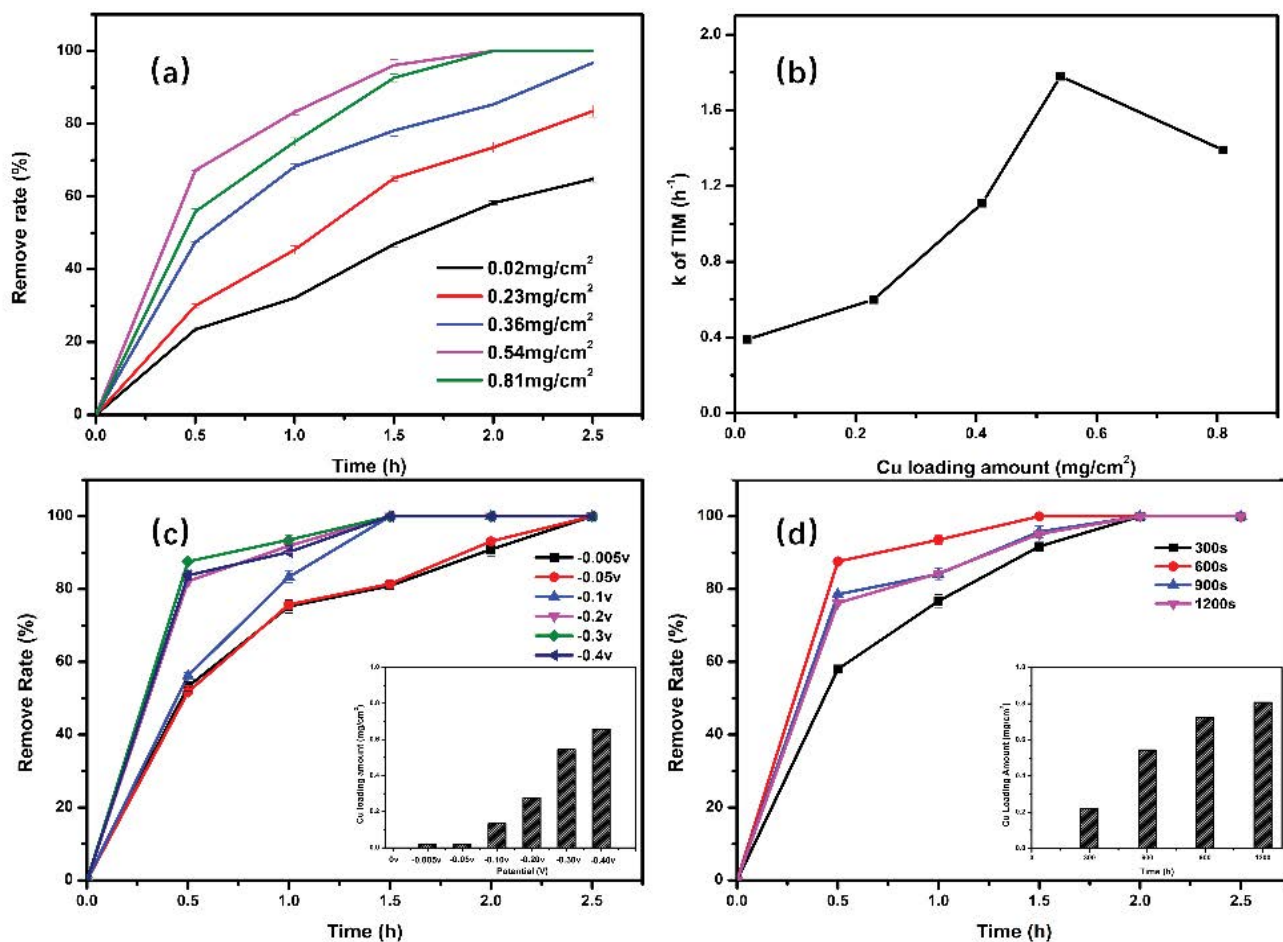
Fig. 4. (a) Effect of Cu loading amount on EC reduction of TIM, (b) kinetics of Cu loading amount on EC reduction of TIM, (c) EC reduction of TIM with deposition time of 600 s and deposition potential from –0.005 to –0.4 V, and (d) removal efficiency of TIM with deposition potential of –0.3 V, following deposition time.

Cheng et al. found that the direct electrochemical reduction at the carbon electrode surface could not promote reductive dechlorination within –1.1 V vs. SCE because hydrogen gas escaped relatively easily from the surface [42]. By contrast, the modified Cu/ACF electrode exhibited the unique property to promote deiodination of TIM due to the ability of Cu to absorb hydrogen into its lattice and to maintain a high surface concentration of hydrogen. Hence, the electroreduction of TIM at –1.0 V on the carbon fiber electrode may be attributed to the reducing cathode potentials using that significantly enhanced direct electron transfer on its surface.

Furthermore, acidic pH is usually beneficial to the removal of pollutants in the EC reduction system because of the presence of H^+ acidic ions improves the formation of free radicals (such as H) [44,45]. Therefore, the acidic environment easily controls the evolution of oxygen to enhance the overall current efficiency, thus promoting the direct and indirect reduction of organic pollutants on the cathode. Although TIM is insoluble in acidic media, it can easily be adsorbed on the surface of activated carbon under acidic conditions. Due to the loading of Cu nanoparticles, a large number of radicals were produced on the surface of Cu/

ACF electrodes, which further accelerated the TIM removal. However, excessive H^+ ions can cause the loss of metal oxides loaded onto the particle electrode, thereby affecting the catalytic effect. It can be concluded that weak acid conditions are beneficial in improving the TIM removal.

To investigated the influence of pH value for TIM removing efficiency, EC reduction of TIM was performed under different pH values (3–11) without any other condition changing. The pH value of the reaction system was adjusted with 0.1 M sodium hydroxide solution and 0.1 M sulfuric acid solution. As shown in Fig. 5, the electrochemical adsorption enhanced reduction of TIM has an excellent removal effect (96.12%) over a wide pH value range. Additionally, during the EC reduction process, although the pH value fluctuates, the total increase/decrease value is less than 1.

3.4. Proposed mechanism for EC reduction of TIM

Due to the difficulty of TIM removing, there are few published papers focused on TIM reduction. As an advanced pollution processing technology, a proposed mechanism for EC reduction of TIM was reported in literatures [46]. The first step of the EC reduction of these species can also

potentially proceed via the classical pathway (reactions 5 and 6) or TIM can be first reduced to CH_2I_2 and the iodine atom $^\bullet I$ (reaction 7):

$$2^\bullet I \rightarrow I_2 \tag{3}$$

$$I_2 + H_2O \rightarrow I^- + HOI + H^+ \tag{4}$$

$$CHI_3 + e \rightarrow I^- + {}^\bullet CHI_2 \tag{5}$$

$${}^\bullet CHI_2 + e + H^+ \rightarrow CH_2I_2 \tag{6}$$

$$CHI_3 + e + H^+ \rightarrow {}^\bullet I + CH_2I_2 \tag{7}$$

The iodine atoms produced from the TIM EC reduction can dimerize to form I_2 (reaction 3) rapidly. The generated I_2 is able to form HOI and I^- ion that are detected on the ring (reaction 4), which undergoes disproportionation readily. Alternatively, the $^\bullet I$ via the EC reduction of TIM on the aq. can react with organic species (for instance, resorcinol or DOM). These reactions will consume the EC-produced $^\bullet I$, thus resulting in the decrease of the iodide production and the formation of I-containing reaction products [11]. Further studies need to be carried out to establish the identities in view of potentially extremely high toxicity of I-DBPs and related compounds [47–49]. Examination of the possible formation of triiodide ions, which can decrease currents associated with the oxidation of free iodide on the ring, indicates that as a result of the absence of free iodide at the initiation of the examined reactions and the low concentrations of this anion and molecular iodine formed via the EC reduction of the examined I-DBPs, the formation of triiodide ion is likely to be largely precluded, given the relatively low equilibrium constant of triiodide formation ($k = 729$) [50].

4. Conclusion

For high-efficiency TIM removing, a catalytic granular electrode (Cu/ACF) was designed by loading Cu
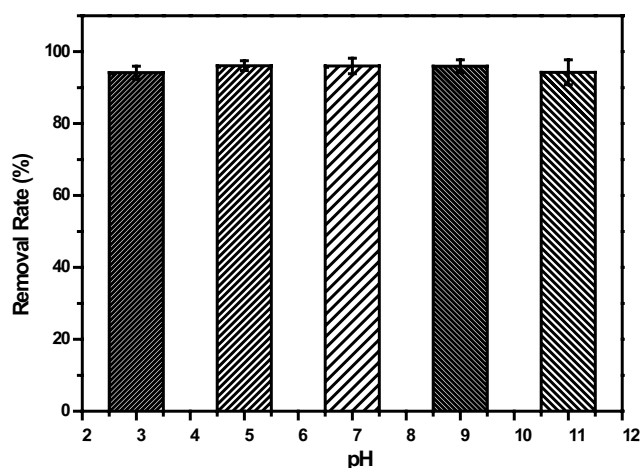
Fig. 5. Effect of initial pH value for the removal efficiency of TIM.

nanoparticles on ACF substrate. The Cu/ACF electrode showed high electrochemical reduction activity on TIM removal in a 3D electrochemical system and achieved 99% removal of TIM. The polycrystalline Cu particles dispersed evenly on the carbon fiber with ca. 50 nm in diameter, which enhanced both the direct electron transfer and indirect atomic H* function for TIM reduction. In addition, the indirect atomic H* function made a major contribution to TIM removal. The removal of TIM followed the pseudo-first order kinetics. The rate constant k remained low when the applied potential was lower than –1.0 V and was largely increased at –1.0 V. Accordingly, the electrochemical reduction of TIM was supposed to proceed with direct mechanism at potentials more positive than –1.0 V, and with indirect mechanism via reaction with atomic H* at potentials more negative than –1.0 V. In the range from –1.0 to –1.9 V, the electrochemical reduction efficiency was greatly increased and was hardly affected by solution pH value. The adsorption enhanced electrochemical reduction provided an efficient approach for environmental TIM reduced removing with low-cost materials under mild conditions.

References

[1] Y. Bichsel, U. von Gunten, Formation of iodo-trihalomethanes during disinfection and oxidation of iodide-containing waters, Environ. Sci. Technol., 34 (2000) 2784–2791.

[2] Y. Bichsel, U. von Gunten, Oxidation of iodide and hypoiodous acid in the disinfection of natural waters, Environ. Sci. Technol., 33 (1999) 4040–4045.

[3] S.W. Krasner, H.S. Weinberg, S.D. Richardson, S.J. Pastor, R. Chinn, M.J. Sclimenti, G.D. Onstad, A.D. Thruston, Occurrence of a new generation of disinfection byproducts, Environ. Sci. Technol., 40 (2006) 7175–7185.

[4] G. Hua, D.A. Reckhow, Comparison of disinfection byproduct formation from chlorine and alternative disinfectants, Water Res., 41 (2007) 1667–1678.

[5] S.D. Richardson, Environmental mass spectrometry: emerging contaminants and current issues, Anal. Chem., 80 (2008) 4373–4402.

[6] S.D. Richardson, F. Fasano, J.J. Ellington, F.G. Crumley, K.M. Buettner, J.J. Evans, B.C. Blount, L.K. Silva, T.J. Waite, G.W. Luther, A.B. McKague, R.J. Miltner, E.D. Wagner, M.J. Plewa, Occurrence and mammalian cell toxicity of iodinated disinfection byproducts in drinking water, Environ. Sci. Technol., 42 (2008) 8330–8338.

[7] D.B. Jones, A. Saglam, A. Triger, H. Song, T. Karanfil, I-THM formation and speciation: preformed monochloramine versus prechlorination followed by ammonia addition, Environ. Sci. Technol., 45 (2011) 10429–10437.

[8] S.D. Richardson, New disinfection by-product issues: emerging DBPs and alternative routes of exposure, Global NEST J., 7 (2005) 43–60.

[9] B. Cancho, F. Ventura, M. Galceran, A. Diaz, S. Ricart, Determination, synthesis and survey of iodinated trihalomethanes in water treatment processes, Water Res., 13 (2000) 3380–3390.

[10] T.Y. Zhang, B. Xu, C.Y. Hu, Y.L. Lin, L. Lin, T. Ye, F.X. Tian, A comparison of iodinated trihalomethane formation from chlorine, chlorine dioxide and potassium permanganate oxidation processes, Water Res., 14 (2014) 0043–1354.

[11] C.E. Jones, L.J. Carpenter, Solar photolysis of CH_2I_2, CH_2ICl, and CH_2IBr in water, saltwater, and seawater, and seawater, Environ. Sci. Technol., 39 (2005) 6130–6137.

[12] J. Criquet, S. Allard, E. Salhi, C.A. Joll, A. Heitz, U. von Gunten, Iodate and iodo-trihalomethane formation during chlorination of iodide-containing waters: role of bromide, Environ. Sci. Technol., 46 (2012) 7350–7357.

[13] S. Allard, J.W.A. Charrois, C.A. Joll, A. Heitz, Simultaneous analysis of 10 trihalomethanes at nanogram per liter levels in water using solid-phase microextraction and gas chromatography mass-spectrometry, J. Chromatogr. A, 1238 (2012) 15–21.

[14] M.J. Farré, K. Doederer, W. Gernjak, Y. Poussade, H. Weinberg, Disinfection by-products management in high quality recycled water, Water Sci. Technol. Water Supply, 12 (2012) 573–579.

[15] K.M.S. Hansen, R. Zortea, A. Piketty, S.R. Vega, H.R. Andersen, Photolytic removal of DBPs by medium pressure UV in swimming pool water, Sci. Total Environ., 443 (2013) 850–856.

[16] Y. Xiao, R. Fan, L. Zhang, J. Yue, R.D. Webster, T. Lim, Photodegradation of iodinated trihalomethanes in aqueous solution by UV 254 irradiation, Water Res., 49 (2014) 275–285.

[17] Y. Xiao, L. Zhang, J. Yue, R.D. Webster, T. Lim, Kinetic modeling and energy efficiency of UV/H_2O_2 treatment of iodinated trihalomethanes, Water Res., 75 (2015) 259–269.

[18] T.C. Wang, C.K. Tan, M.C. Liou, Degradation of bromoform and chlorodibromomethane in a catalyzed H_2-water system, Bull. Environ. Contam. Toxicol., 41 (1988) 563–568.

[19] C.S. Criddle, P.L. McCarty, Electrolytic model system for reductive dehalogenation in aqueous environments, Environ. Sci. Technol., 25 (1991) 973–978.

[20] L.J. Matheson, P.G. Tratnyek, Reductive dehalogenation of chlorinated methanes by iron metal, Environ. Sci. Technol., 28 (1994) 2045–2053.

[21] N.M. Marković, C.A. Lucas, H.A. Gasteiger, P.N. Ross, Bromide adsorption on Pt(100): rotating ring-Pt(100) disk electrode and surface X-ray scattering measurements, Surf. Sci., 365 (1996) 229–240.

[22] N. Sonoyama, T. Sakata, Electrochemical continuous decomposition of chloroform and other volatile chlorinated hydrocarbons in water using a column type metal impregnated carbon fiber electrode, Environ. Sci. Technol., 33 (1999) 3438–3442.

[23] G.V. Korshin, M.D. Jensen, Electrochemical reduction of haloacetic acids and exploration of their removal by electrochemical treatment, Electrochim. Acta, 47 (2001) 747–751.

[24] D.E. Kimbrough, I.H. Suffet, Electrochemical removal of bromide and reduction of THM formation potential in drinking water, Water Res., 36 (2002) 4902–4906.

[25] N. Sonoyama, S. Seike, T. Sueoka, T. Sakata, Electrochemical decomposition of ppb level trihalomethane in tap water, J. Appl. Electrochem., 33 (2003) 1049–1055.

[26] J. Ghilane, M. Delamar, M. Guilloux-Viry, C. Lagrost, C. Mangeney, and P. Hapiot, Indirect reduction of aryldiazonium salts onto cathodically activated platinum surfaces: formation of metal-organic structures, Langmuir, 21 (2005) 6422–6429.

[27] X. Li, D. Heryadi, A.A. Gewirth, Electroreduction activity of hydrogen peroxide on Pt and Au electrodes, Langmuir, 21 (2005) 9251–9259.

[28] V.N. Trang, N.P. Dan, L.D. Phuong, B.X. Thanh, Pilot study on the removal of TOC, THMs, and HAAs in drinking water using ozone/UV-BAC, Desal. Water Treat., 52 (2014) 990–998.

[29] S. Tang, X. Wang, H. Yang, Y.F. Xie, Haloacetic acid removal by sequential zero-valent iron reduction and biologically active carbon degradation, Chemosphere, 90 (2013) 1563–1567.

[30] J. Radjenović, M.J. Farré, Y. Mu, W. Gernjak, J. Keller, Reductive electrochemical remediation of emerging and regulated disinfection byproducts, Water Res., 46 (2012) 1705–1714.

[31] L. Altamar, L. Fernández, C. Borras, J. Mostany, H. Carrero, B. Scharifker, Electroreduction of chloroacetic acids (mono-, di- and tri-) at polyNi(II)-tetrasulfonated phthalocyanine gold modified electrode, Sens. Actuators, B, 146 (2010) 103–110.

[32] A. Li, X. Zhao, Y. Hou, H. Liu, L. Wu, J. Qu, The electrocatalytic dechlorination of chloroacetic acids at electrodeposited Pd/Fe-modified carbon paper electrode, Appl. Catal., B, 111–112 (2012) 628–635.

[33] X. Zhao, A. Li, R. Mao, H. Liu, J. Qu, Electrochemical removal of haloacetic acids in a three-dimensional electrochemical reactor with Pd-GAC particles as fixed filler and Pd-modified carbon paper as cathode, Water Res., 51 (2014) 134–143.

[34] T. Li, J. Farrell, Reductive dechlorination of trichloroethene and carbon tetrachloride using iron and palladized-iron cathodes, Environ. Sci. Technol., 34 (2000) 173–179.

[35] X. Wang, P. Ning, H. Liu, J. Ma, Dechlorination of chloroacetic acids by Pd/Fe nanoparticles: effect of drying method on metallic activity and the parameter optimization, Appl. Catal., B, 94 (2010) 55–63.

[36] S. Yuan, M. Tian, X. Lu, Electrokinetic movement of hexachlorobenzene in clayed soils enhanced by Tween 80 and β-cyclodextrin, J. Hazard. Mater., 137 (2006) 1218–1225.

[37] S. Yuan, X. Mao, and A.N. Alshawabkeh, Efficient degradation of TCE in groundwater using Pd and electro-generated H_2 and O_2: a shift in pathway from hydrodechlorination to oxidation in the presence of ferrous ions, Environ. Sci. Technol., 46 (2012) 3398–3405.

[38] P.M.L. Bonin, P. Edwards, D. Bejan, C.C. Lo, N.J. Bunce, A.D. Konstantinov, Catalytic and electrocatalytic hydrogenolysis of brominated diphenyl ethers, Chemosphere, 58 (2005) 961–967.

[39] B.P. Chaplin, M. Reinhard, W.F. Schneider, C. Schüth, J.R. Shapley, T.J. Strathmann, C.J. Werth, Response to comment on "critical review of pd-based catalytic treatment of priority contaminants in water", Environ. Sci. Technol., 46 (2012) 11469–11470.

[40] X. Wang, Q. Wu, H. Ma, C. Ma, Z. Yu, Y. Fu, X. Dong, Fabrication of PbO_2 tipped Co_3O_4 nanowires for efficient photoelectrochemical decolorization of dye (reactive brilliant blue KN-R) wastewater, Sol. Energy Mater. Sol. Cells, 191 (2019) 381–388.

[41] Q. Shen, Z. Chen, X. Huang, M. Liu, G. Zhao, High-yield and selective photoelectrocatalytic reduction of CO_2 to formate by metallic copper decorated Co_3O_4 nanotube arrays, Environ. Sci. Technol., 49 (2015) 5828–5835.

[42] I-F. Cheng, F. Quintus, K. Nic, Electrochemical dechlorination of 4-chlorophenol to phenol, Environ. Sci. Technol., 31 (1997) 1074–1078.

[43] Y. Wu, L. Gan, S. Zhang, B. Jiang, H. Song, W. Li, Y. Pan, A. Li, Enhanced electrocatalytic dechlorination of para-chloronitrobenzene based on Ni/Pd foam electrode, Chem. Eng. J., 316 (2017) 146–153.

[44] F.C. Moreira, R.A.R. Boaventura, E. Brillas, V.J.P. Vilar, Electrochemical advanced oxidation processes: a review on their application to synthetic and real wastewaters, Appl. Catal., B, 202 (2017) 217–261.

[45] W. Zhang, D. Xie, X. Li, W. Ye, X. Jiang, Y. Wang, W. Liang, Electrocatalytic removal of humic acid using cobalt-modified particle electrodes, Appl. Catal., A, 559 (2018) 75–84.

[46] J. Ma, M. Yan, A.M. Kuznetsov, A.N. Masliy, G. Ji, G.V. Korshin, Rotating ring-disk electrode and quantum-chemical study of the electrochemical reduction of monoiodoacetic acid and iodoform, Environ. Sci. Technol., 49 (2015) 13542–13549.

[47] G. Ding, X. Zhang, A picture of polar iodinated disinfection byproducts in drinking water by (UPLC/)ESI-tqMS, Environ. Sci. Technol., 43 (2009) 9287–9293.

[48] M. Yang, X. Zhang, Comparative developmental toxicity of new aromatic halogenated DBPs in a chlorinated saline sewage effluent to the marine polychaete *Platynereis dumerilii*, Environ. Sci. Technol., 47 (2013) 10868–10876.

[49] J. Liu, X. Zhang, Comparative toxicity of new halophenolic DBPs in chlorinated saline wastewater effluents against a marine alga: halophenolic DBPs are generally more toxic than haloaliphatic ones, Water Res., 65 (2014) 64–72.

[50] J.A. Warner, W.H. Casey, R.A. Dahlgren, Interaction kinetics of I_2 (aq) with substituted phenols and humic substances, Environ. Sci. Technol., 34 (2000) 3180–3185.